

Kinetics study of CH₂OO Criegee intermediate reaction with SO₂, (H₂O)₂, CH₂I₂ and I atom using OH laser induced fluorescence

Yiqiang Liu,^{a,b} Fenghua Liu,^a Siyue Liu,^{a,b} Dongxu Dai,^a Wenrui Dong,^{*a} and Xueming Yang^{*a}

^a State Key Laboratory of Molecular Reaction Dynamics, Dalian Institute of Chemical Physics, Chinese Academy of Sciences, Dalian, Liaoning 116023, China.

^b School of Physics and Optoelectric Engineering, Dalian University of Technology, Dalian, Liaoning 116023, China.

Author Information

Corresponding Author

[*wrdong@dicp.ac.cn](mailto:wrdong@dicp.ac.cn), xmyang@dicp.ac.cn

I. First order kinetics of CH₂OO

The loss of CH₂OO comes from its self-reaction as well as reacting with other radicals. Some previous experiments showed the decay traces of CH₂OO can be described by first-order process.^{1,2,3} The differential rate equation for loss of CH₂OO can be written as follows:

$$\frac{d[\text{CH}_2\text{OO}]}{dt} = k_{2a}[\text{CH}_2\text{I}][\text{O}_2] - K_{\text{obs}}[\text{CH}_2\text{OO}] \quad (\text{S1})$$

where K_{obs} is the total loss rate of CH₂OO. By combining eqn (s1) and eqn (6) in the main text, time dependant [OH] can be described as follows:

$$[\text{OH}] = \frac{K_d}{K_s} \left([\text{CH}_2\text{OO}]_0 + \frac{K_{2a}[\text{CH}_2\text{I}]_0}{(K_{2a} - K_{\text{obs}})} \right) \exp(-K_{\text{obs}}t) - \frac{K_d K_{2a}[\text{CH}_2\text{I}]_0}{K_s(K_{2a} - K_{\text{obs}})} \exp(-K_2t) \quad (\text{S2})$$

According to eqn (S2), OH signals as the function of time can be fitted with the difference of two exponentials:

$$S_{\text{OH}} = C_0 \exp(-K_{\text{obs}}t) - C_1 \exp(-K_2t) \quad (\text{S3})$$

II. Comparison of different fitting methods for various concentration of O₂.

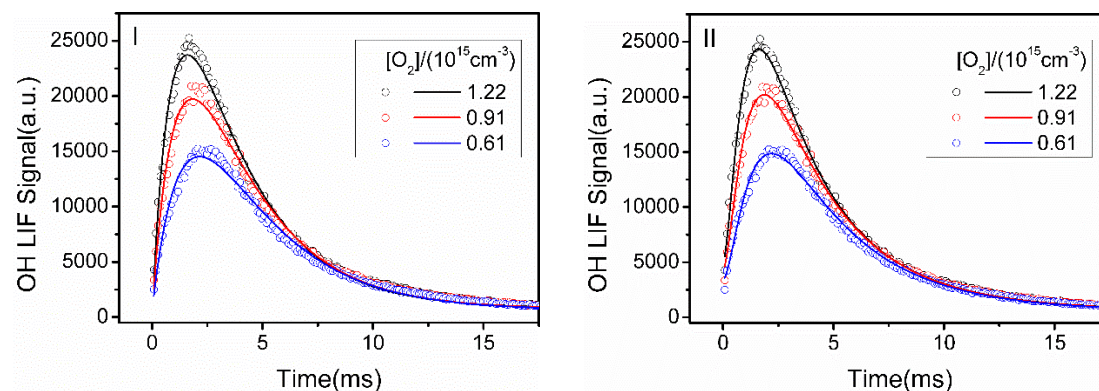


Fig. S1. The OH decay traces were acquired in different concentration of O₂, which were fitted either by applying eqn (S3) with the first order loss of CH₂OO considered I) or eqn (7) with both the first and second order loss of CH₂OO considered II). All the decay traces were taken at 10 Torr total pressure.

In low concentration of O₂ (0.61×10^{15} - 1.22×10^{15} molecule cm⁻³), the comparison of the OH decay traces fitted with different methods, either the first order or both the first and second order kinetics of CH₂OO considered, was shown in Fig. S1. Fig. S1 I) showed that the difference of two exponentials could not fit the time traces of OH very well. That may be the reason why Liu et al.

($[O_2] < 1.63 \times 10^{15}$ molecule cm^{-3}) added another exponential in their fitting⁴. In Fig. S1 II), some discrepancies between the original data and the fitted lines appeared at the time around 2.5 ms. The OH decay traces could not be well fitted with either the first order or both the first and second order kinetics of CH_2OO , which implicated there may be some secondary reactions at conditions that the O_2 concentration is low (SOM of ref.5).

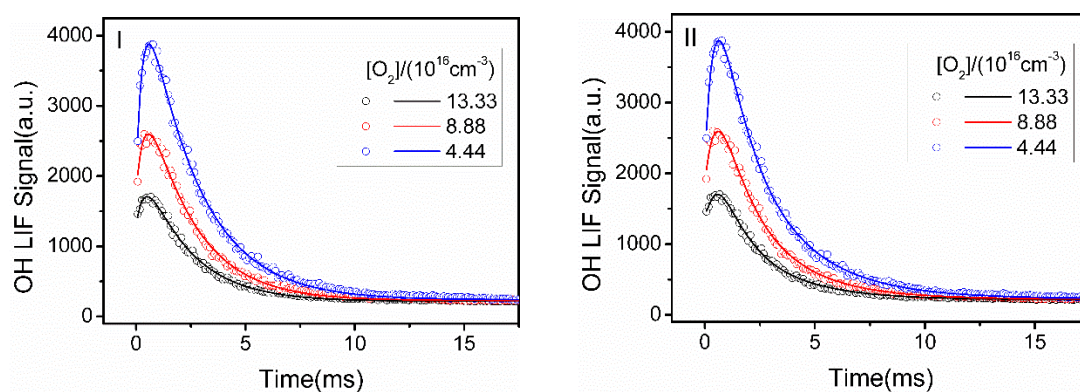


Fig. S2. The OH decay traces were acquired in different concentration of O_2 , which is similar to Fig. S1, but different O_2 concentration was used. The OH decay traces were fitted either by applying eqn (S3) with the first order loss of CH_2OO considered I) or eqn (7) with both the first and second order loss of CH_2OO considered II).

In comparison, within high concentration range of O_2 (4.44×10^{16} - 1.33×10^{17} molecule cm^{-3}), the OH decay traces could be well fitted with the difference of two exponentials, in consistence with Chao et al.³ ($[O_2] > 3.2 \times 10^{17}$ molecule cm^{-3}) and Lewis et al.¹ ($[O_2] \sim 2 \times 10^{17}$ molecule cm^{-3}), who showed the time traces of CH_2OO could be well fitted using the first-order kinetics of CH_2OO . The OH decay traces could also be well fitted via applying eqn (7) with both the first and second order kinetics of CH_2OO considered.

The total flow rate in the flow tube reactor was kept constant and the change of the concentration of O_2 was balanced by that of Ar. The OH detection efficiency changes with O_2 concentration since O_2 and Ar have different quench factors for the OH ($A^2\Sigma^+$).^{6,7} In Fig. S1 the peak intensity of the OH signals increases with $[O_2]$ concentration, while Fig. S2 shows the reverse trends; the former may be chiefly caused by some processes which competed with O_2 to consume CH_2I , while the lower detection efficiency of OH may be largely responsible for the latter.

III. Comparison of results with and without considering the second order kinetics of CH_2OO

Fig. S3 I) shows the fitting of OH decay traces in the presence of various concentration of SO_2 with eqn (S3), the same data as the ones used in Fig. 1. The fitted K_{obs} plotted against SO_2 concentrations was shown in Fig S3 II). For comparison, K_{obs} derived from fitting the OH decay traces with the first order kinetics of CH_2OO was shown in red and those with both the first and second order kinetics of CH_2OO was shown in black. The linear fit of K_{obs} against $[SO_2]$ yielded the rate coefficient of $CH_2OO + SO_2$. The rate coefficient obtained with

inclusion of the second order kinetics of CH₂OO in the analysis is slightly larger, as the correction of the K_{obs} increases while decreasing the SO₂ concentration.

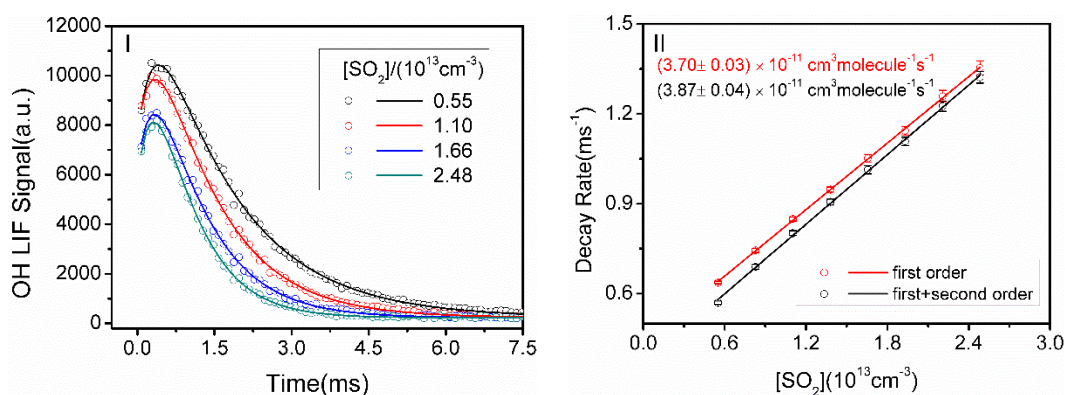


Fig. S3. I) OH decay traces in the presence of various concentrations of SO₂, the same data in Fig. 1. For comparison, eqn (S3) was used in fitting of the OH decay traces. II) The fitted values of K_{obs} were plotted against the concentration of SO₂, and the slopes of the linear fittings give the CH₂OO + SO₂ bimolecular reaction rate coefficient. K_{obs} was derived from fittings based on either first order (red) or both the first and second order (black) kinetics of CH₂OO.

Table S1. Summary of A_0 , A_1 , K_2 , K_{obs} , σ (standard deviation of K_{obs}) and R^2 , which were derived from fitting the OH decay traces with inclusion of the second order kinetics of CH₂OO by applying eqn (7). During the analysis, $[CH_2OO]_M$ was fixed to 5.24×10^{12} molecules/cm³.* The plot of K_{obs} against $[SO_2]$ was shown in Fig. 2.

$[SO_2]^a$	A_0	A_1	K_2/s^{-1}	K_{obs}/s^{-1}	σ/s^{-1}	R^2
2.48	32005.1	26399.1	3158.1	1317.3	18.9	0.9989
2.21	35555.0	28727.0	3034.3	1220.2	16.6	0.9990
1.93	28422.3	22139.2	3019.6	1103.5	13.9	0.9991
1.66	27651.2	21567.5	2961.9	1009.0	13.5	0.9989
1.38	26746.2	20071.3	2856.7	902.1	9.6	0.9993
1.10	29514.4	21864.8	2698.9	798.0	8.2	0.9993
0.83	28465.6	21515.3	2512.4	685.7	7.6	0.9991
0.55	28173.1	20642.0	2534.6	566.1	5.8	0.9992

a. Unit in 10^{13} molecules/cm³

*We first floated the $[CH_2OO]_M$ during the fitting, and then obtained the listed values by performing the second round of fittings using the averaged value of $[CH_2OO]_M$.

Table S2. Summary of C_0 , C_1 , K_2 , K_{obs} , σ (standard deviation of K_{obs}) and R^2 , which were derived from fitting the OH decay traces with the first order kinetics of CH_2OO by applying eqn (S3). The plot of K_{obs} against $[SO_2]$ was shown in Fig. S3.

$[SO_2]^a$	C_0	C_1	K_2/s^{-1}	K_{obs}/s^{-1}	σ/s^{-1}	R^2
2.48	22386.6	16946.6	2940.7	1353.1	22.8	0.9989
2.21	24353.1	17716.3	2829.3	1258.9	19.7	0.9989
1.93	18931.8	12780.5	2939.6	1143.4	13.9	0.9991
1.66	18023.3	12074.5	2975.3	1051.6	12.6	0.9989
1.38	16953.9	10432.8	2980.9	947.0	8.3	0.9993
1.10	18292.1	10841.9	2869.2	848.8	7.1	0.9993
0.83	17134.7	10374.4	2708.0	743.9	6.7	0.9990
0.55	16653.8	9456.1	3122.7	636.7	4.2	0.9991

a. Unit in 10^{13} molecules/ cm^{-3}

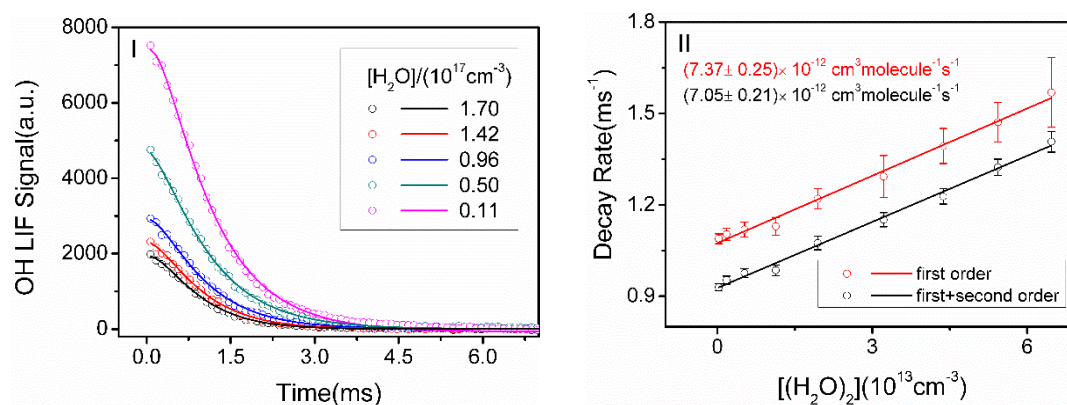


Fig. S4. I) The OH decay traces in presence of various concentration of H_2O , the same data in Fig. 3. For comparison, eqn (S3) was used in fitting of the OH decay traces. II) The fitted values of K_{obs} were plotted against the concentration of $(H_2O)_2$, and the slopes of the linear fittings were responded to the $CH_2OO + (H_2O)_2$ bimolecular reaction rate coefficient. K_{obs} was derived from fittings based on either first order (red) or both the first and second order (black) kinetics of CH_2OO .

Table S3. Summary of A_0 , A_1 , K_2 , K_{obs} , σ (standard deviation of K_{obs}) and R^2 , which were derived from fitting the OH decay traces with inclusion of the second order kinetics of CH_2OO by applying eqn (7). During the analysis, $[CH_2OO]_M$ was fixed to 1.65×10^{13} molecule/cm³. The plot of K_{obs} against $[(H_2O)_2]$ was shown in Fig. 4.

$[H_2O]^a$	A_0	A_1	K_2/s^{-1}	K_{obs}/s^{-1}	σ/s^{-1}	R^2
1.84	9041.6	6649.2	4265.3	1368.7	32.2	0.9962
1.68	9200.3	6563.9	4345.3	1291.1	25.4	0.9975
1.51	9389.8	6664.6	4276.9	1196.5	24.1	0.9973
1.30	9595.7	6762.0	3957.8	1118.3	21.8	0.9974
1.01	11305.2	7892.4	4214.9	1048.1	21.1	0.9974
0.77	13370.6	9207.0	4009.1	958.1	17.2	0.9979
0.52	17868.8	12277.6	4015.3	949.8	13.5	0.9987
0.31	23881.4	23881.4	4086.5	929.2	12.6	0.9988
0.12	29179.6	29179.6	4117.8	906.2	11.4	0.9989

a. Unit in 10^{17} molecules/cm⁻³

Table S4. Summary of C_0 , C_1 , K_2 , K_{obs} , σ (standard deviation of K_{obs}) and R^2 , which were derived from fitting the OH decay traces with the first order kinetics of CH_2OO by applying eqn (S3). The plot of K_{obs} against $[(H_2O)_2]$ was shown in Fig. S4.

$[H_2O]^a$	C_0	C_1	K_2/s^{-1}	K_{obs}/s^{-1}	σ/s^{-1}	R^2
1.84	5023.2	3077.8	2608.1	1569.3	114.3	0.9955
1.68	4537.0	2315.8	2814.9	1471.9	64.8	0.9971
1.51	4580.8	2267.8	2742.3	1393.4	57.5	0.9971
1.30	4507.0	2184.2	2371.8	1293.2	69.1	0.9967
1.01	4806.1	1880.9	3141.8	1220.8	33.1	0.9969
0.77	5496.0	1960.3	2852.4	1130.4	29.4	0.9974
0.52	7276.2	2514.3	2900.8	1119.3	23.8	0.9982
0.31	9664.5	3350.1	3187.1	1104.4	19.5	0.9982
0.12	11847.3	4411.6	3322.4	1089.6	16.1	0.9985

a. Unit in 10^{17} molecules/cm⁻³

Table S5. Summary of A_0 , A_1 , K_2 , K_{obs} , σ (standard deviation of K_{obs}) and R^2 , which were derived from fitting of the OH decay traces with inclusion of the second order kinetics of CH_2OO by applying eqn (7). The plot of K_{obs} against $[CH_2I_2]$ was shown in Fig. 5. The photolysis radiation pulse energy were a) 40mJ/cm², b) 80mJ/cm², c) 160mJ/cm² respectively.

a)

$[CH_2I_2]^a$	A_0	A_1	$[CH_2OO]_M^b$	K_2/s^{-1}	K_{obs}/s^{-1}	σ/s^{-1}	R^2
4.66	9669.8	7742.4	0.56	2576.2	113.8	3.5	0.9978
9.52	24206.6	19021.6	1.15	2606.6	170.4	3.5	0.9986
14.39	35711.2	28749.5	1.74	3326.4	212.3	3.5	0.9989
18.64	42461.0	33609.5	2.25	3567.3	262.9	4.9	0.9984
22.21	46464.8	36779.0	2.69	4041.1	270.2	5.0	0.9985
26.51	50669.7	39011.8	3.20	4358.2	331.1	6.6	0.9980

b)

$[CH_2I_2]^a$	A_0	A_1	$[CH_2OO]_M^b$	K_2/s^{-1}	K_{obs}/s^{-1}	σ/s^{-1}	R^2
4.66	26430.0	19809.6	1.13	2954.0	131.1	2.9	0.9990
9.52	58602.5	43648.7	2.30	3487.8	190.9	3.1	0.9992
14.39	81866.2	58433.9	3.48	4123.3	267.8	5.2	0.9985
18.64	93762.9	62378.3	4.50	4624.9	327.2	6.2	0.9984
22.21	100463.8	65672.7	5.38	5205.9	363.7	6.2	0.9987
26.51	108724.1	68871.3	6.40	5699.3	435.7	8.3	0.9982

c)

$[CH_2I_2]^a$	A_0	A_1	$[CH_2OO]_M^b$	K_2/s^{-1}	K_{obs}/s^{-1}	σ/s^{-1}	R^2
4.66	68330.1	49780.6	2.26	2769.9	128.8	5.2	0.9970
9.52	122611.3	80166.6	4.61	4052.5	247.4	5.2	0.9983
14.39	154958.8	91576.5	6.95	5068.1	353.5	6.2	0.9986
18.64	179301.3	95181.0	9.00	5633.4	484.9	7.7	0.9987
22.21	176005.7	90123.3	10.76	6485.8	558.4	8.2	0.9989
26.51	180914.0	83792.4	12.80	6716.6	609.0	9.6	0.9987

a. Unit in 10¹⁴ molecules/cm³ b. Unit in 10¹³ molecules/cm³

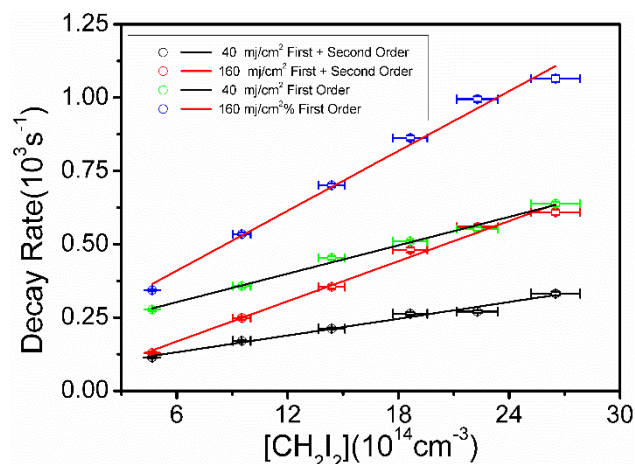


Fig S5. The decay rates K_{obs} were plotted against CH_2I_2 concentration. The green and black open circles were the fitted values of K_{obs} , which were derived from fitting the data obtained with photolysis pulse energy of 40 mj/cm^2 , either by applying eqn (S3) with first order loss of CH_2OO considered (green) or eqn (7) with both the first and second order loss of CH_2OO considered (black). The linear fits of those two sets of data were shown in black lines. Similarly, The blue and red open circles were the fitted values of K_{obs} , which was derived from fitting the data obtained with photolysis pulse energy of 160 mj/cm^2 , either by applying eqn (S3) with first order loss of CH_2OO considered (blue) or by eqn (7) with both the first and second order loss of CH_2OO considered (red). The linear fits of those two sets of data were shown in red lines.

The rate coefficients obtained with inclusion of the second order kinetics of CH_2OO in the analysis is slightly smaller, which was caused by the fact that the correction of the K_{obs} increases while increasing the CH_2I_2 concentration. Since $[CH_2OO]$ is proportional to $[CH_2I_2]$, the self-reaction of CH_2OO will be more important as the $[CH_2I_2]$ increases, which resulted in the increased correction of K_{obs} as mentioned above.

Reference

- ¹ T. R. Lewis, M. A. Blitz, D. E. Heard and P. W. Seakins, *Phys Chem Chem Phys*, 2015, **17**, 4859-4863.
- ² M. C. Smith, C. H. Chang, W. Chao, L. C. Lin, K. Takahashi, K. A. Boering and J. J. M. Lin, *J Phys Chem Lett*, 2015, **6**, 2708-2713.
- ³ W. Chao, J. T. Hsieh, C. H. Chang and J. J. M. Lin, *Science*, 2015, **347**, 751-754.
- ⁴ Y. D. Liu, K. D. Bayes and S. P. Sander, *J Phys Chem A*, 2014, **118**, 741-747.
- ⁵ O. Welz, J. D. Savee, D. L. Osborn, S. S. Vasu, C. J. Percival, D. E. Shallcross and C. A. Taatjes, *Science*, 2012, **335**, 204-207.
- ⁶ P. Hogan and D. D. Davis, *J Chem Phys*, 1975, **62**, 4574-4576.
- ⁷ A. E. Bailey, D. E. Heard, P. H. Paul and M. J. Pilling, *J Chem Soc Faraday T*, 1997, **93**, 2915-2920.